Characterization of metabolomic profile associated with metabolic improvement after bariatric surgery in subjects with morbid obesity

Magali Palau-Rodriguez[a,b], SaraTulipani[a,c], Anna Marco-Ramell[a,b], Antonio Miñarro[d], Olga Jauregui[a,e], Raul Gonzalez-Dominguez[a,b], Alex Sanchez-Pla[d,f], Bruno Ramos-Molina[c,g], Francisco J Tinahones[c,g], Cristina Andres-Lacueva[a,b] *

a. Biomarkers & Nutrimetabolomic Lab, Nutrition, Food Science and Gastronomy Dept, XaRTA, INSA-UB, Campus Torribera, Pharmacy and Food Science Faculty, University of Barcelona, 08028, Barcelona, Spain

b. CIBER Fragilidad y Envejecimiento Saludable [CIBERfes], Instituto de Salud Carlos III [ISCIII], Madrid, Spain

c. Biomedical Research Institute [IBIMA], Service of Endocrinology and Nutrition, Malaga Hospital Complex [Virgen de la Victoria], Campus de Teatinos s/n, Malaga, Spain

d. Genetics, Microbiology and Statistics Department, Biology Faculty, University of Barcelona, 08028, Barcelona, Spain

e. Scientific and Technological Centres of the University of Barcelona (CCIT-UB), 08028 Barcelona, Spain

f. Statistics and Bioinformatics Unit, Vall d'Hebron Institut de Recerca [VHIR], Barcelona, Spain

g.CIBER Fisiopatología de la Obesidad y Nutrición [CIBERobn], Instituto de Salud Carlos III [ISCIII], Barcelona, Spain

Corresponding author:

*Cristina Andres-Lacueva

Biomarkers & Nutrimetabolomic Lab, Nutrition & Food Science Dept, XaRTA, INSA,

CIBERfes Pharmacy and Food Science Faculty, University of Barcelona, 08028, Spain.

Phone: (+34) 934034840

Fax: (+34) 934035931

E-mail address: candres@ub.edu

Abstract

The exact impact of bariatric surgery in metabolically "healthy" (MH) or "unhealthy" (MU) phenotypes for the study of the metabolic improvement is still unknown.

We applied an untargeted LC-ESI-TripleTOF –MS- driven metabolomics approach in serum samples from 39 patients with morbid obesity (MH and MU) 1, 3 and 6 months after bariatric surgery. Multiple factor analysis, along with correlation and enrichment analyses were carried out to distinguish those metabolites associated with metabolic improvement.

Hydroxy-propionic acids, medium-/long-chain hydroxy-fatty acids and bile acid -glucuronides were the most discriminative biomarkers of response between MH and MU phenotypes. Hydroxy-propionic (hydroxyphenyllactic-related) acids, amino acids and glycerolipids were the most significant clusters of metabolites altered after bariatric surgery in MU ($p<0.001$). MU and MH changes after surgery towards a common metabolic state already 3 months after surgery. We observed a negative correlation with changes in waist circumference and cholesterol levels with metabolites of lipid metabolism. Glycaemic variables were correlated with hexoses, which, in turn, correlated with gluconic acid and amino acid metabolism. Finally, we noted that hydroxyphenyllactic acid was associated with amino acid and lipid metabolism.

Microbial metabolism of amino acid and BA glucuronidation pathways may be the key points of metabolic rearranges after surgery.

Keywords: Untargeted metabolomics, microbiota metabotype, bariatric surgery, obesity, metabolically healthy, indole metabolites, mass spectrometry, hydroxyphenyllactic

Abbreviations:

AU, arbitrary unit; BA, bile acid; BCAA, branched-chain amino acid; BMI, body mass index; BP, blood pressure; c-HDL, high-density lipoprotein cholesterol; c-LDL, low-density lipoprotein cholesterol; CRP, C-reactive protein; CVD, cardiovascular disease; DBP, diastolic

blood pressure; DG, diglyceride; ESI-, electrospray operating in negative ionization mode; ESI+, electrospray operating in positive ionization mode; FDR, false discovery rate; FXR, farnesoid-X receptor; GGT, gamma glutamyl transferase; GOT, glutamic-oxaloacetic transaminase; GPT, glutamate-pyruvate transaminase; HbA1c, glycated haemoglobin A1; HOMA-IR index, insulin resistance calculated by homeostatic model assessment index; LC, liquid chromatography; LPE, lysophosphoethanolamine; MFA, multiple factor analysis; MH, metabolically healthy; MS, mass spectrometry; MU, metabolically unhealthy; PC, phosphatidylcholine; PCA, principal component analysis; Phe-Phe, phenylalanine-phenylalanine; QC, quality control; qTOF, quadrupole time-of-flight; SBP, systolic blood pressure; sPLS-DA, sparse partial least-squares discriminant analysis; TG, triglyceride; TGR5, G-protein-coupled receptor; VLDL, very low-density lipoprotein.

Introduction

Obesity is predictive of all-cause mortality and increases the risk of developing metabolic-related diseases such as type 2 diabetes. Obesity is associated with insulin resistance, dyslipidaemia, hypertension and high cardiometabolic risk [1].

Paradoxically, 10–30 % of people with obesity are characterized by low cardiometabolic risk – higher insulin sensitivity, normal blood pressure, lower lipid levels of triglycerides (TG) and low-density lipoproteins, and higher levels of high-density lipoproteins – and thus they are defined metabolically healthy (MH) [2]. Hence, apart from confounders such as age, gender, ethnicity and lifestyle, being or not being MH depends on insulin resistance or the number of metabolic abnormalities present in the individual [3]. These subjects present a lower risk of mortality and of developing metabolic complications [4].

Despite several attempts to describe the mechanisms of metabolic balance in MH obesity, such as those based on inflammatory response [5], visceral adipose tissue regulation or diet/lifestyle [6], the door is still open to achieve the complete understanding of the metabolic health in obesity. Therefore, a change in the study of this paradigm is required to work out the causes of the existence of diverse metabolic profiles in obesity, but especially which specific pathways are involved.

Studying the metabolic changes after the employment of a weight loss strategy such as bariatric surgery may be a tool to unveil insights into metabolic deregulation. Several studies have reported that bariatric surgery is a metabolic modifier, from the dissipation of metabolic syndrome status a few days after the intervention to the remission of type 2 diabetes [7].

The metabolome – the set of metabolites in a biological sample – mirrors the products of the genome, transcriptome and proteome, and reflects any environmental or endogenous manifestations [8]. A comprehensive metabolic profiling of a human serum could provide an

exhaustive view of the evolution of the subjects after surgery [9]and unveil the connection between obesity and their related complications [10].

To date, few metabolomics approaches have been used to study the metabolic consequences of the current strategies for weight loss. Among these, a targeted metabolomics approach is dominant, focused on the quantification of specific groups of metabolites, for instance amino acids [11,12], acylcarnitines [12] and phospholipids [13]. Thus, the use of untargeted metabolomics for a non-hypothesis-driven approach may expand the assessment of the onset of metabolic improvements after a weight loss intervention underlying unknown mechanisms involved. The potential use of metabolomics in the biomedical field has increased the discovery of new biomarkers of prognosis or diagnosis of a disease [14].

The aim of this work is to identify serum metabolites associated with metabolic improvement in subjects with morbid obesity after undergoing bariatric surgery. To this end, we adopted an untargeted metabolomics approach to analyse serum samples of subjects with MH and metabolically unhealthy (MU) obesity both before bariatric surgery intervention and one, three and six months later through liquid chromatography coupled to triple quadrupole time-of-flight mass spectrometry (HPLC-qTOF-MS).

Material and Methods

The protocol was approved by the local Ethics and Research Committee (Hospital Universitario Virgen de la Victoria, Malaga) and all participants provided written informed consent.

Subjects and study design

Serum samples from 39 patients with morbid obesity (body mass index (BMI) > 40 kg/m^2) (> 10-year history of obesity who underwent bariatric surgery (n= 26 roux-en-Y gastric bypass; n= 13 sleeve gastrectomy) were collected before and 1, 3 and 6 months after surgery at the Virgen de la Victoria University Hospital and Carlos Haya Hospital (Malaga, Spain).

Subjects were stratified according to their degree of metabolic syndrome, as defined by the Adult Treatment Panel III criteria [15]: metabolically healthy (MH) subjects with ≤ 2 criteria (n=21) and metabolically unhealthy (MU) subjects with ≥ 3 criteria (n=18).

All the patients were adults (between 19 and 59 years old) and they comprised 27 females and 12 males. The exclusion criteria were the intake of antidiabetic, corticosteroid, or antibiotic drugs, the presence of acute or chronic infection, a history of alcohol abuse or drug dependence and a history of cancer. Other treatments, including anti-inflammatory, antihypertensive and anti-cholesterolemic agents, were recorded.

Anthropometric and biochemical parameters

Anthropometric and biochemical parameters were measured in each period of time using standardized techniques, as previously described [16–18]. In this work we report: a) anthropometric markers: body weight, BMI, waist circumference, hip circumference and waist-hip index; b) markers of glucose regulation: glycated haemoglobin A1c (HbA1c), plasma concentrations of fasting glucose, fasting insulin and calculated Homeostatic Model Assessment (HOMA-IR index=fasting insulin x fasting glucose/22.5 arbitrary units); c) blood pressure markers (BP): diastolic and systolic blood pressure; d) blood lipid markers: total cholesterol (CHOL), very low-density lipoprotein (VLDL), low-density lipoprotein (c-LDL), high-density lipoprotein cholesterol (c-HDL) and TG; and e) liver enzyme activities: gamma glutamyl transferase (GGT), glutamic-oxaloacetic transaminase (GOT) and glutamate-pyruvate transaminase (GPT); and f) C-reactive protein (CRP).

Serum Metabolomic Analysis

Sample Treatment and Data Acquisition

Fasting morning serum was stored at -80 ºC until analysis. Serum samples (50 µL) were subjected to an in-plate hybrid extraction for deproteinization and phospholipid removal with

solid-phase extraction, as described previously [19]. Liquid chromatography (LC) was performed on a Shimadzu Nexera X2 series HPLC system (Kyoto, Japan) using a 50 x 2.1 mm, 5 μm (Waters) Atlantis T3 reverse phase column, with a sample injection volume of 5 μL. A linear gradient elution was performed with a binary system consisting of [A] Milli-Q water 0.1% HCOOH (v/v) and [B] methanol (v/v), at a constant flow rate of 600 μL min^{-1}. The gradient elution (v/v) of [B] used was as follows (time, min; B, %): (0, 0), (2, 0), (4.5, 85), (7, 100), (9.9, 100), (10, 0), (13, 0). The HPLC system was online coupled with a hybrid quadrupole-TOF mass spectrometer TripleTOF 6600 System (AB Sciex, Toronto, Ontario, Canada) equipped with a Turbo Spray IonDrive™ source operating in positive (ESI+) or negative (ESI-) ion electrospray modes. Full data acquisition was performed by scanning from 70 to 850 m/z in both ionization modes. LC-MS data were acquired in two successive batches of analysis and the sequences of injections were randomized in order to avoid possible bias. Three types of quality control (QC) were included in the injection plate design to check for the analytical quality grade: QC1, Milli-Q water samples; QC2, aqueous solution of a standard metabolite mix (5 ppm final standard concentration, described in [20] and QC3, reinjected selected biological samples within the same batch. The QC samples were analysed throughout the run, every 20 injections, to provide a measurement of the stability and performance of the system and evaluate the quality of the acquired data. Information Dependent Acquisition was performed in high-sensitivity and low-cycle time mode, recording masses with an ion count greater than 500 cps, not excluding former target ions, excluding isotopes within 4 Da, with an ion tolerance of 50 ppm, a maximum of seven spectra of candidate ions per cycle and with a dynamic background substract.

Standards and reagents

Internal standard mix of glycocholic acid-(glycine 1-^{13}C) and 1-O-stearoyl-sn-glycero-3-phosphocholine (negative control); external standards mix of acetyl-d3-L-carnitine, indole-3-acetic-2,2-d2 acid (Sigma-Aldrich, St Louis, MO) and QC metabolite standard mix were

prepared as previously described[20]. 2-hydroxy-hexanoic acid, 3-(4-hydroxyphenyl)-2-hydroxypropanoic acid, 3-(4-hydroxyphenyl)-propanoic acid, 3-hydroxy-dodecanoic acid, 3-hydroxy-octanoic acid, 3-hydroxy-tetradecanoic acid, 4-hydroxy-butyric acid, acetylcarnitine, caffeine, choline, citric acid, creatine, docosapentaenoic acid (osbond acid), docosatetraenoic acid (adrenic acid), dodecanoic acid (lauric acid), gluconic acid, hexoses, indole-3-carboxaldehyde, indolelactic acid, isocitric acid, L-arginine, L-citrulline, L-glutamate, L-histidine, L-leucine, L-ornithine, L-tryptophan, L-tyrosine, octadecatrienoic acid (linolenic acid), palmitoylmonoglyceride, phe-phe, retinol, tetradecanoic acid (miristic acid), theobromine and uric acid (Sigma, St. Louis, MO) and octadecenoylcarnitine and octadecadienylcarnitine (Larodan, Solna, Sweden) were used to confirm the identity of metabolites.

Data analysis and metabolite identification

Mass extraction and alignment of the peaks were performed using MarkerView™ 1.3.0.1 software (AB Sciex); parameters were optimized separately for positive and negative ionization modes (Table S-1). The subsequent analyses were executed in R version 3.3.2, unless otherwise noted.

Data were filtered out to remove any ion that did not appear in more than 20% of the samples of each group separately [21]. Data were log-transformed and Pareto-scaled for multivariate analysis [22].

Due to the potential effect of age [23], gender [24] and type of surgery [25] on the metabolome, data were adjusted by these variables in all statistical analyses.

Paired t-tests were used to identify discriminant features at each time point (6 months (T6), 3 months (T3) and 1 month (T1)) with respect to the baseline (T6–T0, T3–T0 and T1–T0) for the MH and MU group separately. To control the false discovery rate (FDR) associated with multiple hypothesis testing, *p*-values were adjusted to allow a maximum 5% probability of false-positive detection based on the Benjamini-Hochberg procedure [26]. A two-way hierarchical

cluster analysis based on Pearson correlation and Ward's distance method was performed to determine clusters of mass features originating from the same metabolite and thereby reducing the queried masses (PermutMatrix 1.9.3 software). Levels of evidence in the annotation of discriminant metabolites were assigned in accordance with Metabolomics Standards Initiative criteria [27]. Putatively annotated compounds were carried out by matching mass features with mass spectral databases (Human Metabolome Database [28], Metlin [29], MetFrag [30]) with a mass error tolerance of ±10 mDa (assigning a level 2 of the evidence in the identification). When peak chromatographic and MS responses of the identified metabolites matched with peak chrompatographic and MS responses of commercial reference standards level 1 of evidence in the identification was assigned.

Multivariate analyses were applied to the identified metabolites to recognize those most responsible for the changes at each time point. Initially, an exploratory analysis was performed through multiple factor analysis (MFA), taking into account each single time point (*FactoMineR* R package)[31]. Afterwards, a sparse partial least squares discriminant analysis (sPLS-DA) was used to distinguish the most discriminative metabolites of MH and MU in T6–T0, T3–T0 and T1–T0 (*spls* R package) [32]. The sparsity (*eta*) and number of hiding components (*K*) were chosen using a ten-fold cross-validation procedure and the predictability of the models was calculated on a leave-one-out basis. Principal components analysis (PCA) and orthogonal projections to latent structures discriminant analysis (OPLS-DA) were used to visualize the separation of the groups. Finally, linear mixed models were employed to obtain the effect of the interaction time x metabolic state.

Pearson correlation analysis was carried out between log-normalized metabolite levels and anthropometric/clinical variables to evaluate the relationship between the metabolite change with the metabolic improvement for each increment of time. Only those correlations of discriminant metabolites at T3–T0, with *p*-values adjusted by multiple testing by the FDR < 0.1 and correlation coefficients > |0.5|, were visualized (Cytoscape 3.5.1.). MFA was also

performed with clinical variables and the discriminative metabolites of MH/MU in T3–T0 to show the relation between these variables.

Enrichment analysis was performed using the bioinformatics tool ChemRich (Chemical Similarity Enrichment Analysis for Metabolomics). The ChemRich statistical approach compares chemical similarities using the Medial Subject Headings database and Tanimoto chemical similarity coefficients to cluster metabolites into non-overlapping chemical groups. *P*-values are obtained by employing the Kolmogorov-Smirnov test using the created clusters and adjusted by the FDR [33].

Results

Anthropometric and clinical parameters

The characteristics of the subjects are presented in Table S-2. MH and MU were balanced in terms of gender, age and anthropometric parameters. At baseline, MU presented higher levels of fasting glucose, HOMA-IR, c-LDL and CHOL (p-value < 0.05). In general, after the surgery the aforementioned variables normalize, already observed 1 month after the intervention. Table S-3 shows the evolution of anthropometric and clinical parameters in both groups after surgery. At 3 months after surgery, seven of the MU group were still "unhealthy" and three of the MH group had crossed the line of "unhealthy" obesity. Six months after the initial point, five patients from the MU group were still "unhealthy" and four of the MH group had changed to being "unhealthy".

The availability of the serum samples before surgery and 1, 3 and 6 months after surgery was as follows: MH: 21, 20, 20 and 17, respectively and MU: 18, 16, 17 and 15, respectively.

Data acquisition quality

The analytical quality was first examined through a PCA displaying the classification of serum samples, confirming that no batches were overlapping, along with the absence of carryover in

QC and the detection of no outliers in positive and negative ionization modes (Figure S-1). The quality of the hybrid extraction was checked by monitoring the internal standards in the chromatogram. LC-MS analytical stability was evaluated by controlling external standards over time. As a result, one sample in the positive ionization mode and other in negative ionization mode did not pass the analytical quality and therefore they were removed. As shown in Table S-4, metabolite components of QC met the quality criteria proposed for the metabolomics analysis protocol: retention time shifts ≤ 0.05 min, mass accuracy deviations < 10 mDa and peak areas with CV < 25%.

Selection and identification of discriminatory metabolites related to metabolic improvement

A first selection of the most discriminative features between groups and time points was performed using univariate analyses. From the initial 3000 features obtained in each ionization mode, the only features that met the criteria ($p < 0.05$) were considered for identifying metabolites. The complete list of identified metabolites and their fold changes is available in Table S-5. Metabolites lacking chemical annotation were not considered for subsequent analyses.

MFA was applied to all identified metabolites irrespective of which time period was statistically significant. The first two dimensions explained 22.47% of the total variance. Figure 1 shows the mean evolution of both groups converging to a common point over time, observed 3 months after surgery, corresponding to the origin of the MFA score plot. Global differences after the surgery are shown in Figure S-2 and the separation of MH and MU in each time point is represented in Figure S-3.

Figure 1. Projection of the *individual mean* (metabolically healthy (MH) and metabolically unhealthy (MU)) for each period of time onto the global analysis, based on the identified metabolites in positive and negative operating modes. The scatter plot was created with the first two dimensions of the Multiple Factor Analysis (MFA). Periods of time are represented by red, green, blue and pink dots corresponding to the baseline (T0), 1 month, 3 months and 6 months after the surgery, respectively, and linked by a black line with the partial positions of each point. Grey dots indicate the position of each subject in the scatter plot.

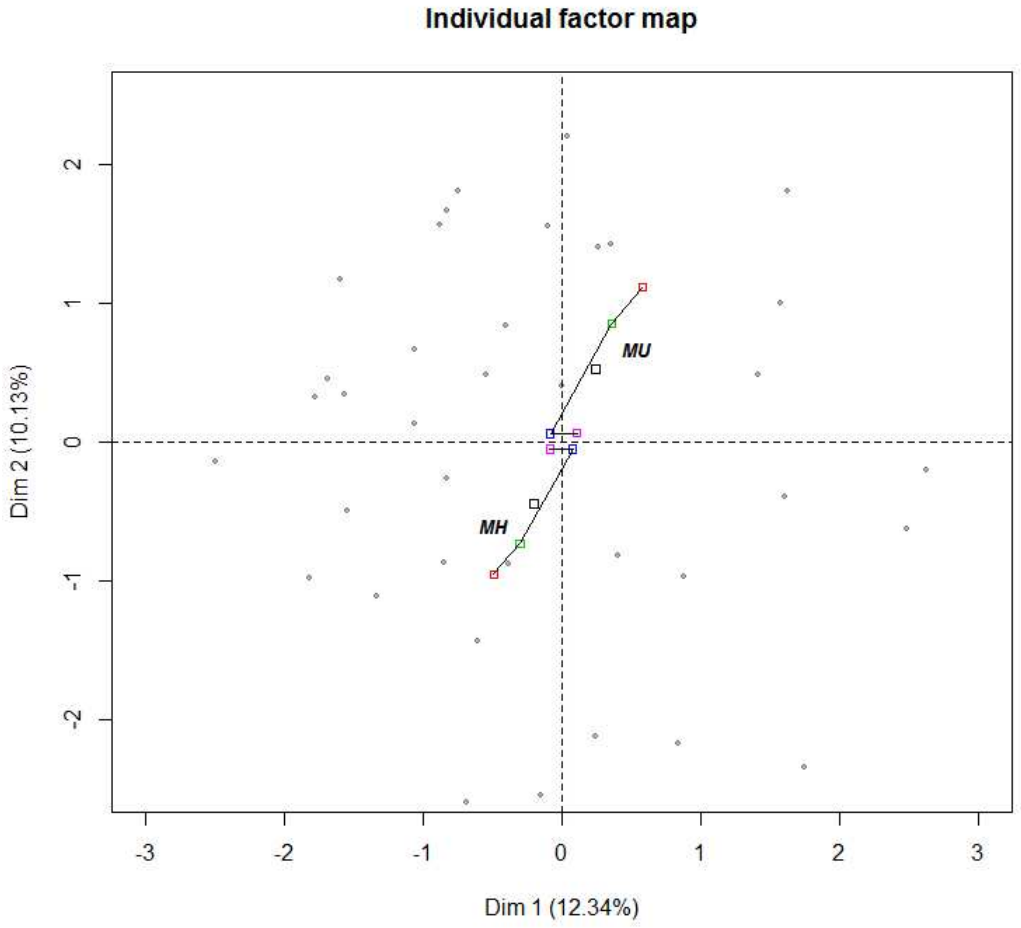

Discriminant metabolites in each increment of time, T6–T0, T3–T0 and T1–T0, were explored through sPLS-DA using the optimal parameters to obtain a minimum classification error (Table S-6). The changes between the groups of patients were mainly acute (T1) and derived from middle-term (T3) adaptations. At 6 months no additional significant metabolites between MH and MU were found (Figure S-4). Discriminant changes in metabolite levels between MH and MU in the convergent point (T3–T0) are shown in Table 1. Briefly, Diglycerides (DGs) and hexoses enabled discrimination between MU and MH in each increment of time, displaying

major fold changes in MU. Acute changes were characterized by modifications in fatty acids, hydroxy fatty acids, amino acids and their microbiota-related compounds (hydroxyphenyl-propionic derivatives). Nevertheless, steroid conjugates and acylcarnitines were mainly discriminative of both groups in the time increment T3–T0. Confirmation of this common steady metabolic state post-surgery in both groups was obtained by comparing whether the levels of the discriminant metabolites in MH were statistically equal to those from MU at 3 months ($p > 0.05$). At 3 months MU group was different from MH group at baseline in terms of tyrosine, leucine, glycochenodeoxycholic acid-3 glucuronide, hydroxy-indolepropanoic acid, indole-3-carboxaldehyde and lysophosphoethanolamines (LPE) metabolites (Table 1).

Enrichment analysis and correlation analysis for metabolic improvement

Correlation between metabolite and clinical variables in T3–T0 showed that changes in waist circumference and cholesterol levels were negatively correlated with LPE and fatty acid metabolism. 3-(4-Hydroxyphenyl)-2-hydroxypropanoic or hydroxyphenyllactic acid was the link between amino acids and lipid metabolism. Changes in 3-(4-Hydroxyphenyl)-2-hydroxypropanoic levels also positively correlated with hexoses. In addition, hexoses associated with glycaemic variables (Figure 2).

Figure 2. Visualization of Pearson correlations between metabolite-metabolite and metabolite-clinical variables (in grey) of the discriminative metabolites between MH and MU in the time incrementT3–T0 (Cytoscape). Only statistical correlations after adjustment of the false discovery rate are shown ($p < 0.1$). Correlations with $r > 0.8$ are represented by thicker lines. Negative correlations are shown in red.

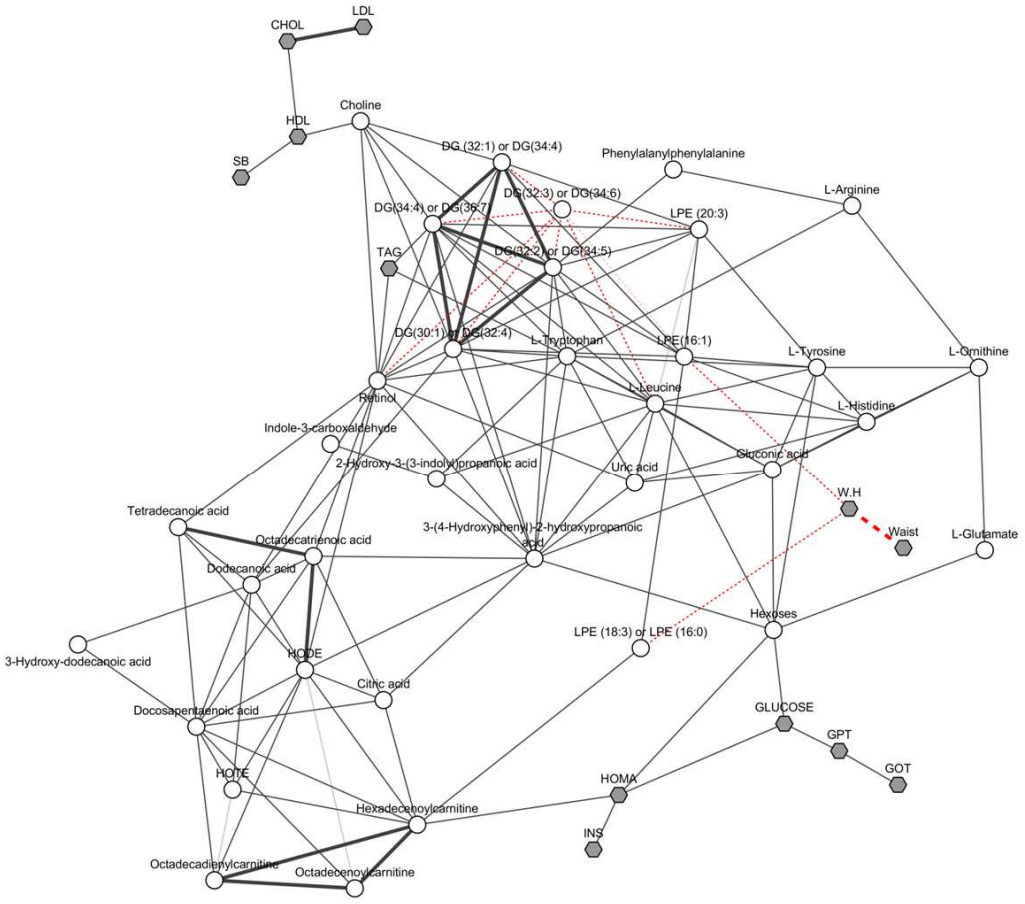

We mapped the 46 discriminative metabolites between groups in the increment T3–T0 in ChemRich, in order to detect those chemical families that were most responsible for the metabolic changes in each group (Table 2). Indoles and derivatives, amino acids, glycerolipids, glycerophospholipids and fatty acids were altered most in MU subjects. On the other hand, not a single chemical family reached statistical significance in the MH group.

MFA of the identified metabolites and clinical variables confirmed the separation of MH and MU in T3–T0 by the first dimension of the scatterplot (Figure 3A, 3C). The third dimension explained the separation between clinical and metabolic variables (Figure 3B). Correlations of the variables with the main dimensions are shown in Figures 3D and E. The first dimension was highly correlated with glycaemia and weight parameters. These variables were hardly overlapped with the acylcarnitines, propionic acids were near CHOL and c-LDL with the DGs (Figure 3E). 3-(4-Hydroxyphenyl)-2-hydroxypropanoic acid presented high correlation with the first dimension and proximity with amino acids and DGs.

Figure 3. Multiple factor analysis (MFA) of clinical variables and identified metabolites in T3–T0. A) Projection of the *mean individual* (metabolically healthy (MH) and metabolically unhealthy (MU)) onto the global analysis, based on the clinical variables and identified metabolites in T3–T0 in positive and negative operating modes. The scatter plot was created with the first two dimensions of the MFA. **B)** The scatter plot was created with the first and the third dimension of the MFA. **C)** Partial axes of each group of variables (clinical, metabolic) in the first two dimensions and position of the health status in the plot. **D)** Correlation circle of variables into the first and second dimensions. Only clinical variables are shown. **E)** Correlation of the variables into the first (x-axis and darkness of the bubbles), second (size of the bubbles) and third (y-axis) dimension of the scatter plot. Clinical, metabolic and health status variables are represented by blue, grey and red, respectively, except in **E** where all the variables are represented by grey.

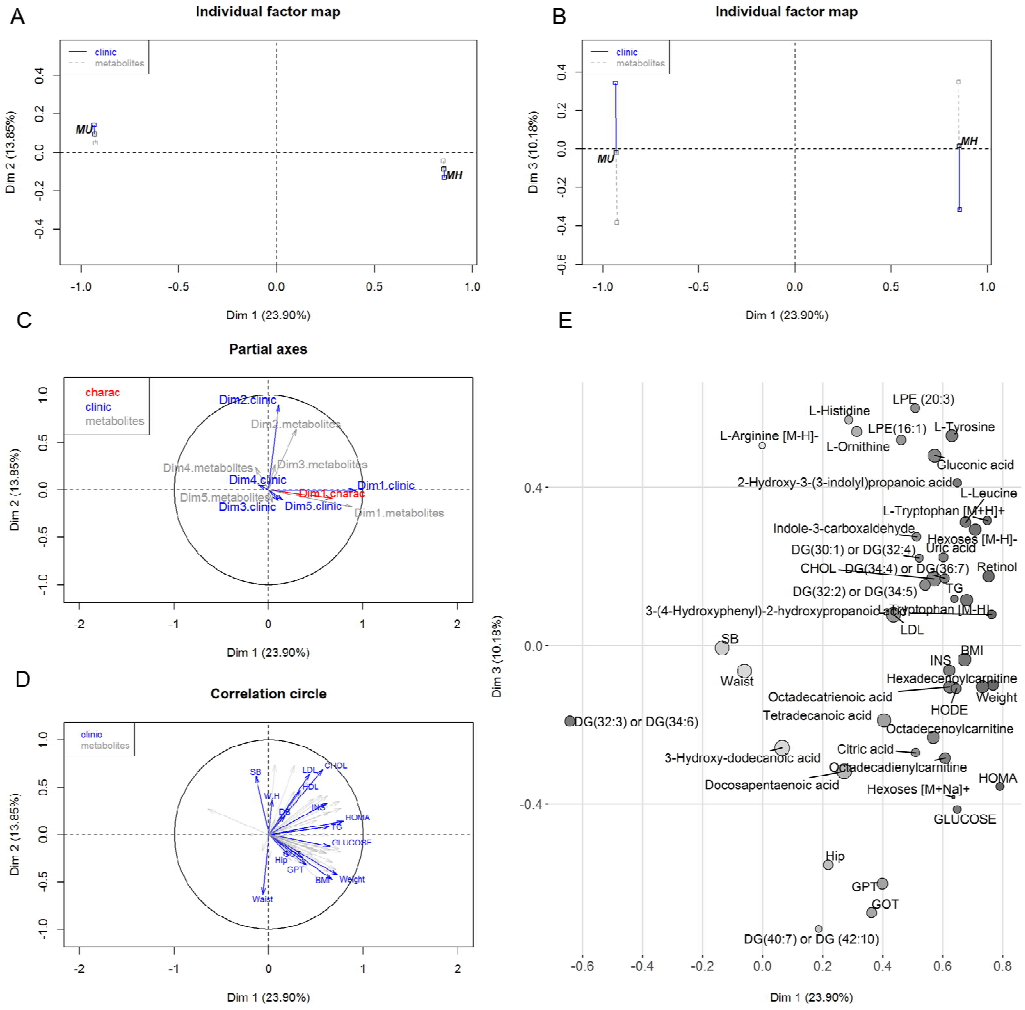

Discussion

Through an untargeted metabolomics approach we explored an integrative global metabolic evolution of patients with morbid obesity after a weight loss intervention. We also identified

metabolic fingerprints of changes in MH and MU after surgery. We observed that microbial related metabolites such as hydroxyl fatty acids, BAs and hydroxy-propionic acid (indole derivatives) are the most important biomarkers to reach a stable metabolic state after bariatric surgery regardless of the health status of the patient at baseline.

MFA revealed that MU and MH changes after surgery towards a common metabolic state 6 months after surgery. In fact, a steady metabolic state was observed in the groups as early as 3 months after the intervention. For this reason, the post-identification analyses have been focused on this time point.

Acute changes in microbial and amino acid-related metabolites

A depletion in amino acid levels was observed as early as 1 month after the intervention. This phenomenon has also been noticed with the use of different strategies for weight loss, and is generally greater after a surgical intervention than after diet/lifestyle changes [12]. High levels of amino acids are a biosignature of subjects with obesity. Out of all the amino acids, branched-chain amino acids (BCAAs) such as leucine, isoleucine and valine, and aromatic amino acids such as tryptophan, tyrosine and histidine, have been described as being correlated with glycaemia disruption [34]. Indeed, BCAAs have been associated with different cardiometabolic complications, from insulin resistance to coronary artery disease [35].

We also identified a drop in the levels of dipeptides after the intervention. Although LC-MS did not allow them to be fully characterized, and a chemical standard was not available, thanks to the MS/MS spectra and databases we have proposed phenylalanine and BCAA derivative dipeptides. However, little is known about their role in obesity and cardiometabolic diseases.

The decrease in the levels of amino acids was also mirrored by changes in gut microbiota metabolism products. We found that indole metabolites were the most important chemical family of metabolites that changes in MU after bariatric surgery. (Hydroxyphenyl-)hydroxypropionic acid and 2-Hydroxy-3-(3-indolyl)propanoic acid are gut microbiota-related

compounds of the amino acid metabolism. Recently the reductive pathway of *Clostridium sporongenes*, a gut bacterium from the phylum Firmicutes, has been demonstrated to produce phenylpropionic acid, hydroxyphenylpropionic acid and indolepropionic acid through the metabolizing of phenylalanine, tyrosine and tryptophan, respectively [36]. Moreover, the degradation of phenylalanine and tyrosine by lactic acid bacteria increases the levels of hydroxyl-propionic acid metabolites [37]. The catabolism of tryptophan produces hydroxyl-indolepropionic acid. A recent study has suggested that the stimulating of indole- derivatives production could promote anti-inflammatory response, improving the mucus layer[38].

Correlation analysis suggested that these microbiota-metabolites could like the metabolism of amino acids, glucose, fatty acid and DGs. Thus, (Hydroxyphenyl-)hydroxypropionic acid and 2-Hydroxy-3-(3-indolyl)propanoic acid could be key in the metabolic regulation after surgery.

On the other side, the increase in the number of BA glucuronides and steroid sulphates suggests the involvement of phase II (detoxifying) glucuronyl- and sulphate-transferase enzymes. Glucuronide conjugates represent up to 10 % of the circulating pool of BAs in healthy individuals. However, conjugated BAs with amino acids are such relatively strong acids that even glucuronidation, which is the major phase II biotransformation pathway for exogenous components such as drugs, remains a minor pathway for endogenous BAs [39].

In the same way, the adaptive changes post-surgery could be responsible for the decrease in bacteria with glucuronidase activity.. In addition, the alteration of dietary patterns, intestinal motility and mucosal hyperplasia post-surgery may contribute to modifying the composition of BAs [40].

How BAs affect the metabolism of an individual has already been described. BAs are known to regulate the metabolism of glucose and energy through the farnesoid-X receptor (FXR) and G-protein-coupled receptor TGR5, respectively [41]. Nevertheless, the biological activity of the different forms of BAs is still unknown. While glycine-conjugated BAs are as efficient as the

unconjugated form in activating FXR, Trottier et al. demonstrated that glucuronide conjugates suppress the biological activity of BAs [42].

Certain studies have attempted to link BAs with metabolic improvement. These studies were mainly targeted approaches based on specific BA structures [43] or the global profile of primary/secondary or conjugated/unconjugated BAs [44], but they excluded those derived from alternative metabolisms such as glucuronidation or sulphatation. Although no significant correlations were observed in T3–T0, we suggest that BAs may be potential biomarkers in regulating the metabolic state of an individual.

Steady changes in lipid and gluconeogenic metabolism

MU subjects present greater changes in levels of lipid metabolism than subjects classified as healthy. In fact, lipid species and derivatives interfere with different metabolic pathways to increase insulin resistance. Our results indicate that there are three interconnected major groups of metabolites that reflect mechanism-induced insulin resistance: fatty acids, DGs and acylcarnitines. It is worth noting that different studies have reported inconsistent trends in specific lipid metabolites and cardiovascular diseases: for instance, diacyl-phosphatidilcholine (PC) C32:1 has been independently associated with increased risk of T2D, and acyl-alkyl- PC C34:3 with a decreased risk [45]. Therefore, each PC, fatty acid or derivate should be considered an entity in itself. Generalizing about the role of a pathway in the development of an unhealthy phenotype could be inaccurate, so a specific emphasis on each lipid structure is required.

A higher delivery of fatty acids to the muscle and liver is associated with lower rates of intracellular fat oxidation and/or the conversion of fatty acids to neutral lipids. The main causes that may contribute to this decontrol are: an excess of caloric intake, defects in adipocyte metabolism, alterations in mitochondrial fatty acid oxidation and inhibition of lipoprotein lipase activity [46]. We noted that from the first month after bariatric surgery, both DGs and fatty acids,

especially long-chain fatty acids and those that are hydroxylated, decreased in MU. 3-hydroxy-octanoic acid and 3-hydroxy-dodecanoic acid increased in MH.

In MH, an increase in the number of long-chain acylcarnitines was observed after surgery. Increases in acylcarnitines after the first month may be caused by incomplete long-chain fatty acid beta-oxidation and an altered tricarboxylic cycle, as already characterized in diabetes. Acetylcarnitine is a product of fatty acid beta-oxidation and glucose oxidation and can be used by the citric acid cycle for energy generation. In the same vein, we also observed the effect of the gluconeogenic metabolism through changes in citric acid, gluconic acid and total hexose metabolites. In MU, levels of citric acid increase, presumably to compensate for the decrease in hexose levels and gluconic acid.

Translating our results into the physiopathology of obesity, these findings may indicate that different metabolic mechanisms may lead to the development of related diseases, from impaired mitochondrial oxidation, reflected by an increase levels of fatty acids, DGs and acylcarnitines, to acute changes in amino acid-related microbiota metabolites and conjugated/unconjugated BA.

Strengths and limitations

The removal of proteins and glycerophospholipids by this validated method has improved the quality of the MS signals for the identification of specific molecules. We were aware that this could provoke the lost of specific groups of metabolites. The interpretation and validation of our results is still limited to the completeness of chemical annotation in databases, the characteristics of LC-MS data and the availability of standards in the market.

To reduce the chance of false-positive findings from the low number of patients enrolled in the study, rigorous statistical strategies were applied. For instance, a strict data mining approach was applied to reduce the dimensionality of the data, and multivariate discriminate analyses

were used to select the most important metabolites in order to classify the groups. It is worth noting that stronger results would be obtained by using an independent validation cohort.

Conclusions

In a nutshell, this study opens new insights into the physiological changes after bariatric surgery toward a distinct metabolic status in humans. Microbial indole-related products, as well as the BA glucuronidation pathway, may be the key in the regulation of metabolic health in subjects with obesity. The great potential of an untargeted metabolomics approach has to be exploited to understand the obesity and metabolic profiles.

Acknowledgement

The authors thank Cristina Plunkett for her collaboration in the study and AB Sciex for the usage of equipment at the Warrington core facility (UK) and software programs. This research was supported by Project PI13/01172 (Plan N de I+D+i 2013-2016), co-funded by ISCII-Subdirección General de Evaluación y Fomento de la Investigación; Project PI-0557-2013, co-funded by Fundación Progreso y Salud, Consejería de Salud y Bienestar Social, Junta de Andalucía, CIBERfes and CIBERobn, co-funded by Fondo Europeo de Desarrollo Regional (FEDER) and MTM2015/64465-C2-1-R (MINECO/FEDER). 2017SGR1546 and 2017 SGR 622 supported by Generalitat de Catalunya's Agency (AGAUR). M.P.-R acknowledged the APIF fellowship [INSA-UB]; ST, AMR and RGD acknowledge the Juan de la Cierva fellowship [MINECO] and BRM acknowledges the Sara Borrell postdoctoral fellowship (CD16/0003).

Conflict of Interest Disclosure

The authors declare no conflict of interest

Supporting Information

The following files are available free of charge at ACS website http://pubs.acs.org:

Figure S-1. Principal component analysis (PCA) score plot of samples (dots): QC1 (Milli-Q water samples), QC2 (aqueous solution of a standard) and QC3 (replicates). ; **Figure S-2.** Group score plot representation of each period of time.; **Figure S-3.** PCA and OPLS-DA score plot representation; **Figure S-4.** Venn diagram of the discriminative metabolites in each increment of time (T1–T0, T3–T0, T6–T0) according to the results of the sPLS-DA; **Table S-1.** Data pre-processing parameters;**Table S-2.** Anthropometric, biochemical and clinical characteristics of metabolically healthy (MH) and unhealthy (MU) individuals before the intervention;**Table S-3.** Anthropometric, biochemical and clinical characteristics of metabolically healthy (MH) and unhealthy (MU) individuals over time;**Table S-4.** Variation in retention time, peak area, peak height and detection mass in aqueous QC2 samples injected in randomized order throughout the analysis;**Table S-5.** Identified metabolites of changes after surgery in metabolically healthy (MH) and metabolically unhealthy (MU) subjects with obesity at each period of time;

Table S-6. Sparse Partial Least Squares discriminant analysis paramaters chosen for each increment of time and % of correct classification.

References

(1) Solomon, C. G.; Manson, J. E. Obesity and Mortality: A Review of the Epidemiologic Data. *Am. J. Clin. Nutr.* **1997**, *66* (4 Suppl), 1044S–1050S.

(2) Wildman, R. P.; Muntner, P.; Reynolds, K.; Mcginn, A. P. The Obese Without Cardiometabolic Risk Factor Clustering and the Normal Weight With Cardiometabolic Risk Factor Clustering. *Arch. Intern. Med.* **2008**, *168* (15), 1617–1624.

(3) Phillips, C. M.; Dillon, C.; Harrington, J. M.; McCarthy, V. J. C.; Kearney, P. M.; Fitzgerald, A. P.; Perry, I. J. Defining Metabolically Healthy Obesity: Role of Dietary and Lifestyle Factors. *PLoS One* **2013**, *8* (10), 1–13.

(4) Primeau, V.; Coderre, L.; Karelis, a D.; Brochu, M.; Lavoie, M.-E.; Messier, V.; Sladek, R.; Rabasa-Lhoret, R. Characterizing the Profile of Obese Patients Who Are Metabolically Healthy. *Int. J. Obes. (Lond).* **2011**, *35* (7), 971–981.

(5) Barbarroja, N.; López-Pedrera, R.; Mayas, M. D.; García-Fuentes, E.; Garrido-Sánchez, L.; Macías-González, M.; El Bekay, R.; Vidal-Puig, A.; Tinahones, F. J. The Obese Healthy Paradox: Is Inflammation the Answer? *Biochem. J.* **2010**, *430* (1), 141–149.

(6) Janiszewski, P. M. P.; Ross, R.; Care, C.; Janiszewski, P. M. P.; Ross, R. Effects of Weight Loss Among Metabolically Healthy Obese Men. *Diabetes Care* **2010**, *33* (9), 1957–1959.

(7) Pories, W. J.; Swanson, M. S.; MacDonald, K. G.; Long, S. B.; Morris, P. G.; Brown, B. M.; Barakat, H. a; deRamon, R. a; Israel, G.; Dolezal, J. M. Who Would Have Thought It? An Operation Proves to Be the Most Effective Therapy for Adult-Onset Diabetes Mellitus. *Ann. Surg.* **1995**, *222* (3), 339-350; discussion 350-352.

(8) Bain, J. R. Targeted Metabolomics Finds Its Mark in Diabetes Research. *Diabetes* **2013**, *62* (2), 349–351.

(9) Tulipani, S.; Griffin, J.; Palau-Rodriguez, M.; Mora-Cubillos, X.; Bernal-Lopez, R. M.; Tinahones, F. J.; Corkey, B. E.; Andres-Lacueva, C. Metabolomics-Guided Insights on Bariatric Surgery versus Behavioral Interventions for Weight Loss. *Obesity* **2016**, *24* (12).

(10) Palau-Rodriguez, M.; Tulipani, S.; Queipo-Ortuño, M. I.; Urpi-Sarda, M.; Tinahones, F. J.; Andres-Lacueva, C. Metabolomic Insights into the Intricate Gut Microbial-Host Interaction in the Development of Obesity and Type 2 Diabetes. *Front. Microbiol.* **2015**, *6* (OCT).

(11) Shah, S. H.; Crosslin, D. R.; Haynes, C. S.; Nelson, S.; Turer, C. B.; Stevens, R. D.; Muehlbauer, M. J.; Wenner, B. R.; Bain, J. R.; Laferr??re, B.; et al. Branched-Chain Amino Acid Levels Are Associated with Improvement in Insulin Resistance with Weight Loss. *Diabetologia* **2012**, *55* (2), 321–330.

(12) Laferrere, B.; Reilly, D.; Arias, S.; Swerdlow, N.; Gorroochurn, P.; Bawa, B.; Bose, M.; Teixeira, J.; Stevens, R. D.; Wenner, B. R.; et al. Differential Metabolic Impact of Gastric Bypass Surgery Versus Dietary Intervention in Obese Diabetic Subjects Despite Identical Weight Loss. *Sci. Transl. Med.* **2011**, *3* (80), 80re2-80re2.

(13) Oberbach, A.; Bergen, M. Von; Blüher, S.; Lehmann, S.; Till, H. Combined Serum Proteomic and Metabonomic Profiling After Laparoscopic Sleeve Gastrectomy in Children and Adolescents. *J. Laparoendosc. Adv. Surg. Tech.* **2012**, *22* (2), 184–188.

(14) Newgard, C. B. Metabolomics and Metabolic Diseases: Where Do We Stand? *Cell Metab.* **2017**, *25* (1), 43–56.

(15) Expert Panel on Detection, Evaluation, and T. of H. B. C. in A. Executive Summary of the Third Report of the National Cholesterol Education Program (NCEP) Expert Panel

on Detection, Evaluation, and Treatment of High Blood Cholesterol in Adults (Adult Treatment Panel III). *JAMA J. Am. Med. Assoc.* **2001**, *285* (19), 2486–2497.

(16) Garrido-Sanchez, L.; Murri, M.; Rivas-Becerra, J.; Ocaña-Wilhelmi, L.; Cohen, R. V.; Garcia-Fuentes, E.; Tinahones, F. J. Bypass of the Duodenum Improves Insulin Resistance Much More Rapidly than Sleeve Gastrectomy. *Surg. Obes. Relat. Dis.* **2012**, *8* (2), 145–150.

(17) Tinahones, F. J.; Queipo-Ortuño, M. I.; Clemente-Postigo, M.; Fernnadez-Garcia, D.; Mingrone, G.; Cardona, F. Postprandial Hypertriglyceridemia Predicts Improvement in Insulin Resistance in Obese Patients after Bariatric Surgery. *Surg. Obes. Relat. Dis.* **2013**, *9* (2), 213–218.

(18) Murri, M.; Insenser, M.; Bernal-Lopez, M. R.; Perez-Martinez, P.; Escobar-Morreale, H. F.; Tinahones, F. J. Proteomic Analysis of Visceral Adipose Tissue in Pre-Obese Patients with Type 2 Diabetes. *Mol. Cell. Endocrinol.* **2013**, *376* (1–2), 99–106.

(19) Tulipani, S.; Llorach, R.; Urpi-Sarda, M.; Andres-Lacueva, C. Comparative Analysis of Sample Preparation Methods to Handle the Complexity of the Blood Fluid Metabolome: When Less Is More. *Anal. Chem.* **2013**, *85* (1), 341–348.

(20) Tulipani, S.; Mora-Cubillos, X.; Jáuregui, O.; Llorach, R.; García-Fuentes, E.; Tinahones, F. J.; Andres-Lacueva, C. New and Vintage Solutions To Enhance the Plasma Metabolome Coverage by LC-ESI-MS Untargeted Metabolomics: The Not-So-Simple Process of Method Performance Evaluation. *Anal. Chem.* **2015**, *87* (5), 2639–2647.

(21) Smilde, A. K.; Van Der Werf, M. J.; Bijlsma, S.; Van Der Werff-Van Der Vat, B. J. C.; Jellema, R. H. Fusion of Mass Spectrometry-Based Metabolomics Data. *Anal. Chem.* **2005**, *77* (20), 6729–6736.

(22) van den Berg, R. a; Hoefsloot, H. C. J.; Westerhuis, J. a; Smilde, A. K.; van der Werf, M. J. Centering, Scaling, and Transformations: Improving the Biological Information Content of Metabolomics Data. *BMC Genomics* **2006**, *7*, 142.

(23) Yu, Z.; Zhai, G.; Singmann, P.; He, Y.; Xu, T.; Prehn, C.; R??misch-Margl, W.; Lattka, E.; Gieger, C.; Soranzo, N.; et al. Human Serum Metabolic Profiles Are Age Dependent. *Aging Cell* **2012**, *11* (6), 960–967.

(24) Bachlechner, U.; Floegel, A.; Steffen, A.; Prehn, C.; Adamski, J.; Pischon, T.; Boeing, H. Associations of Anthropometric Markers with Serum Metabolites Using a Targeted Metabolomics Approach: Results of the EPIC-Potsdam Study. *Nutr. Diabetes* **2016**, *6* (6), e215.

(25) Gralka, E.; Luchinat, C.; Tenori, L.; Ernst, B.; Thurnheer, M.; Schultes, B. Metabolomic Fingerprint of Severe Obesity Is Dynamically Affected by Bariatric Surgery in a Procedure-Dependent Manner. *Am. J. Clin. Nutr.* **2015**, *102* (6), 1313–1322.

(26) Benjamini Yoav, H. Y. Controling the False Discovery Rate: A Practical and Powerful Approach to Multiple Testing. *J. R. Stat. Soc. Ser. B* **1995**, *57* (1), 289–300.

(27) Sumner, L. W.; Amberg, A.; Barrett, D.; Beale, M. H.; Beger, R.; Daykin, C. A.; Fan, T. W.-M.; Fiehn, O.; Goodacre, R.; Griffin, J. L.; et al. Proposed Minimum Reporting Standards for Chemical Analysis Chemical Analysis Working Group (CAWG) Metabolomics Standards Initiative (MSI). *Metabolomics* **2007**, *3* (3), 211–221.

(28) Wishart, D. S.; Jewison, T.; Guo, A. C.; Wilson, M.; Knox, C.; Liu, Y.; Djoumbou, Y.; Mandal, R.; Aziat, F.; Dong, E.; et al. HMDB 3.0-The Human Metabolome Database in 2013. *Nucleic Acids Res.* **2013**, *41* (D1), 801–807.

(29) Smith, C. a; Maille, G. O.; Want, E. J.; Qin, C.; Trauger, S. a; Brandon, T. R.; Custodio, D. E.; Abagyan, R.; Siuzdak, G. METLIN. *Ther. Drug Monit.* **2005**, *27* (6), 747–751.

(30) Wolf, S.; Schmidt, S.; Müller-Hannemann, M.; Neumann, S. In Silico Fragmentation for Computer Assisted Identification of Metabolite Mass Spectra. *BMC Bioinformatics* **2010**, *11* (1), 148.

(31) Abdi, H.; Williams, L. J.; Valentin, D. Multiple Factor Analysis: Principal Component Analysis for Multitable and Multiblock Data Sets. *Wiley Interdiscip. Rev. Comput. Stat.* **2013**, *5* (2), 149–179.

(32) Cao, K. a L.; Boitard, S.; Besse, P. Sparse PLS Discriminant Analysis: Biologically Relevant Feature Selection and Graphical Displays for Multiclass Problems. *BMC Bioinformatics* **2011**, *12* (June), 16.

(33) Barupal, D. K.; Fiehn, O. Chemical Similarity Enrichment Analysis (ChemRICH) as Alternative to Biochemical Pathway Mapping for Metabolomic Datasets. *Sci. Rep.* **2017**, *7* (1), 1–11.

(34) Newgard, C. B.; An, J.; Bain, J. R.; Muehlbauer, M. J.; Stevens, R. D.; Lien, L. F.; Haqq, A. M.; Shah, S. H.; Arlotto, M.; Slentz, C. a.; et al. A Branched-Chain Amino Acid-Related Metabolic Signature That Differentiates Obese and Lean Humans and Contributes to Insulin Resistance. *Cell Metab.* **2009**, *9* (4), 311–326.

(35) Magnusson, M.; Lewis, G. D.; Ericson, U.; Orho-Melander, M.; Hedblad, B.; Engström, G.; Östling, G.; Clish, C.; Wang, T. J.; Gerszten, R. E.; et al. A Diabetes-Predictive Amino Acid Score and Future Cardiovascular Disease. *Eur. Heart J.* **2013**, *34* (26), 1982–1989.

(36) Dodd, D.; Spitzer, M. H.; Van Treuren, W.; Merrill, B. D.; Hryckowian, A. J.; Higginbottom, S. K.; Le, A.; Cowan, T. M.; Nolan, G. P.; Fischbach, M. a.; et al. A Gut Bacterial Pathway Metabolizes Aromatic Amino Acids into Nine Circulating Metabolites. *Nature* **2017**, *551* (7682), 648–652.

(37) Valerio, F.; Lavermicocca, P.; Pascale, M.; Visconti, A. Production of Phenyllactic Acid by Lactic Acid Bacteria: An Approach to the Selection of Strains Contributing to Food Quality and Preservation. *FEMS Microbiol. Lett.* **2004**, *233* (2), 289–295.

(38) Wlodarska, M.; Luo, C.; Kolde, R.; d'Hennezel, E.; Annand, J. W.; Heim, C. E.; Krastel, P.; Schmitt, E. K.; Omar, A. S.; Creasey, E. a.; et al. Indoleacrylic Acid Produced by Commensal Peptostreptococcus Species Suppresses Inflammation. *Cell Host Microbe* **2017**, *22* (1), 25–37.e6.

(39) Werth, M.; Gaunitz, F.; Gebhardt, R. Reply: *Hepatology* **2007**, *45* (4), 1083–1083.

(40) Nakatani, H.; Kasama, K.; Oshiro, T.; Watanabe, M.; Hirose, H.; Itoh, H. Serum Bile Acid along with Plasma Incretins and Serum High-Molecular Weight Adiponectin Levels Are Increased after Bariatric Surgery. *Metabolism.* **2009**, *58* (10), 1400–1407.

(41) Ryan, K. K.; Tremaroli, V.; Clemmensen, C.; Kovatcheva-Datchary, P.; Myronovych, A.; Karns, R.; Wilson-Pérez, H. E.; Sandoval, D. A.; Kohli, R.; Bäckhed, F.; et al. FXR Is a Molecular Target for the Effects of Vertical Sleeve Gastrectomy. *Nature* **2014**, *509* (7499), 183–188.

(42) Trottier, J.; Verreault, M.; Grepper, S.; Monté, D.; Bélanger, J.; Kaeding, J.; Caron, P.; Inaba, T. T.; Barbier, O. Human UDP-Glucuronosyltransferase (UGT)1A3 Enzyme Conjugates Chenodeoxycholic Acid in the Liver. *Hepatology* **2006**, *44* (5), 1158–1170.

(43) Yu, H.; Ni, Y.; Bao, Y.; Zhang, P.; Zhao, A.; Chen, T.; Xie, G.; Tu, Y.; Zhang, L.; Su, M.; et al. Chenodeoxycholic Acid as a Potential Prognostic Marker for Roux-En-Y Gastric Bypass in Chinese Obese Patients. *J. Clin. Endocrinol. Metab.* **2015**, *100* (11), 4222–4230.

(44) Pournaras, D. J.; Glicksman, C.; Vincent, R. P.; Kuganolipava, S.; Alaghband-Zadeh, J.; Mahon, D.; Bekker, J. H. R.; Ghatei, M. a.; Bloom, S. R.; Walters, J. R. F.; et al. The

Role of Bile after Roux-En-Y Gastric Bypass in Promoting Weight Loss and Improving Glycaemic Control. *Endocrinology* **2012**, *153* (8), 3613–3619.

(45) Floegel, A.; Stefan, N.; Yu, Z.; Mühlenbruch, K.; Drogan, D.; Joost, H. G.; Fritsche, A.; Häring, H. U.; De Angelis, M. H.; Peters, A.; et al. Identification of Serum Metabolites Associated with Risk of Type 2 Diabetes Using a Targeted Metabolomic Approach. *Diabetes* **2013**, *62* (2), 639–648.

(46) Erion, D. M.; Shulman, G. I. Diacylglycerol-Mediated Insulin Resistance. *Nat. Med.* **2010**, *16* (4), 400–402.

Table 1. Discriminant serum metabolites between metabolically healthy and metabolically unhealthy subjects in the time increment T3-T0 (in accordance with the results of sPLS-DA[a)]

Potential marker	m/z[b]	Error [mDa]	RT [min]	Assignation	Level[c]	Discriminant[d]			MU (n=18)[e]	MH (n=21)[e]	MU T3 vs MH T0[f]
						T1	T3	T6			
CHO metabolism											
Hexoses	179.0649	-8.8	0.32	[M-H]-	1	√	√	√	-0.19 ± 0.15**	0.00 ± 0.19	
Hexoses	203.0524	0.2	0.31	[M+Na]+					-0.18 ± 0.19*	0.01 ± 0.13	
Gluconic acid	195.0620	-11	0.33	[M-H]-	1	√	√		-0.23 ± 0.23**	-0.07 ± 0.38	
Citric acid	191.0189	0.8	0.79	[M-H]-	1		√		0.20 ± 0.44*	0.39 ± 0.51***	
Amino acids											
L-Tryptophan	203.0819	0.7	3.58	[M-H]-	1		√		-0.53 ± 0.57**	-0.27 ± 0.36	
L-Tryptophan	205.0966	0.6	3.54	[M+H]+					-0.41 ± 0.46**	-0.17 ± 0.36	
L-Tyrosine	180.0662	0.4	0.95	[M-H]-	1		√		-0.50 ± 0.46**	-0.27 ± 0.41**	**
L-Arginine	173.1144	-10	0.30	[M-H]-	1	√	√		-0.12 ± 0.20**	-0.07 ± 0.15	
L-Arginine	175.1183	0.7	0.30	[M+H]+					-0.10 ± 0.24	-0.02 ± 0.15	
L-Citrulline	198.084	0.9	0.31	[M+Na]+	1	√	√		-0.09 ± 0.24	0.06 ± 0.26	
L-Glutamate	146.0581	-12.2	0.32	[M-H]-	1	√	√		-0.12 ± 0.14**	-0.02 ± 0.12	
L-Histidine	154.0707	-8.5	0.31	[M-H]-	1		√		-0.10 ± 0.21	-0.09 ± 0.18	
L-Leucine	130.0869	0.5	0.90	[M-H]-	1		√		-0.41 ± 0.38**	-0.30 ± 0.36*	*
L-Ornithine	131.0878	-5.2	0.33	[M-H]-	1		√		-0.05 ± 0.23	-0.02 ± 0.22	
Dipeptides											
Phenylalanylphenylalanine	313.1553	-0.6	4.06	[M+H]+	1	√	√		-0.39 ± 0.88	-0.25 ± 0.78	
Gamma-glutamyl-L-isoleucine	259.1120	17.9	0.31	[M-H]-	2		√	√	-0.22 ± 0.54	-0.01 ± 0.25	
Acylcarnitines											
Hexadecenoylcarnitine	398.3254	1.1	5.16	[M+H]+	2		√		-0.08 ± 0.66	0.21 ± 0.54	
Octadecadienylcarnitine (linoleyl carnitine)	424.3412	0.9	5.21	[M+H]+	1		√		0.01 ± 0.67	0.15 ± 0.40	

Octadecenoylcarnitine (elaidic carnitine)	426.3565	1.3	5.28	[M+H]+	1		√		0.21 ± 0.59	0.35 ± 0.36***	
Fatty acids											
3-Hydroxy-octanoic acid	159.1017	1	4.88	[M-H]-	1	√	√		-0.09 ± 0.51	0.11 ± 0.46	
3-Hydroxy-dodecanoic acid	215.1647	0.6	5.39	[M-H]-	1	√	√		0.15 ± 0.47	0.22 ± 0.50**	
Hydroxy-octadecatrienoic acid (HOTE)	295.2243	2.5	5.61	[M+H]+	2		√		-0.06 ± 0.30	0.00 ± 0.21	
Hydroxy-octadecadienoic acid (HODE)	301.2119	2.5	6.22	[M+Na]+	2		√		-0.41 ± 0.63*	-0.03 ± 0.48	
Dodecanoic acid (lauric acid)	199.1698	0.6	5.80	[M-H]-	1	√	√		-0.27 ± 0.49	-0.07 ± 0.44	
Tetradecanoic acid (myristic acid)	227.2009	0.8	6.22	[M-H]-	1		√		-0.25 ± 0.45	-0.05 ± 0.44	
Octadecatrienoic acid (linolenic acid)	277.2157	1.6	6.26	[M-H]-	1		√		-0.43 ± 0.59	-0.12 ± 0.54	
Docosapentaenoic acid (osbond acid)	331.2625	0.6	6.54	[M+H]+	1	√	√		0.02 ± 0.61	0.21 ± 0.48**	
Diglycerides											
DG(30:1) or DG(32:4)	561.4482	0.7 or 3.2	8.10	[M+Na/H]+	2	√	√	√	-0.57 ± 0.67*	-0.15 ± 0.46	
DG(32:3) or DG(34:6)	585.4494	-0.5	8.19	[M+Na/H]+	2		√		4.49 ± 2.86**	1.59 ± 3.12	
DG(32:2) or DG(34:5)	587.4647	-0.1	8.18	[M+Na/H]+	2	√	√	√	-0.69 ± 0.65**	-0.27 ± 0.50	
DG(32:1) or DG(34:4)	589.4804	-0.2	8.44	[M+Na/H]+	2	√	√	√	-0.45 ± 0.47**	-0.12 ± 0.31	
DG(34:4) or DG(36:7)	611.4647	-0.1	8.10	[M+Na/H]+	2		√		-0.94 ± 0.76**	-0.46 ± 0.81	
DG(40:7) or DG(42:10)	689.512	-0.5	8.50	[M+Na/H]+	2	√	√		-0.11 ± 0.60	0.03 ± 0.49	
Steroids/Bile acids derivatives											
Glycochenodeoxycholic acid 3-glucuronide	606.3233	4.5	5.25	[M-H2O-H]-	2		√		0.09 ± 0.54	-0.20 ± 1.16	*
Cholic acid glucuronide	583.3073	5.1	5.35	[M-H]-	2		√		0.34 ± 1.73	1.14 ± 1.92**	
Dihydroxyandrostenone sulfate	383.1528	0.6	6.01	[M-H]-	2		√		0.35 ± 0.77	0.47 ± 0.63**	
Microbiota derivatives			0.00								
3-(4-Hydroxyphenyl)-	165.055	0.7	4.88	[M-H]-	1	√	√		0.56 ± 1.91	1.66 ± 2.49**	

propionic acid										
3-(4-Hydroxyphenyl)-2-hydroxypropanoic acid	181.0494	1.2	3.76	[M-H]-	1	√	√	-0.49 ± 0.38**	-0.25 ± 0.38	
2-Hydroxy-3-(3-indolyl)propionic acid	204.0659	0.7	4.31	[M-H]-	1	√	√	-0.53 ± 0.48**	-0.46 ± 0.32***	*
Purine derivatives										
Uric acid	167.0299	-8.8	0.41	[M-H]-	1	√	√	-0.19 ± 0.17**	-0.13 ± 0.13**	
Cofactors and vitamins			0.00							
Retinol	269.2261	0.8	6.29	[M-H20+H]	1	√	√	-0.48 ± 0.50*	-0.10 ± 0.23	
Choline	104.1066	0.4	0.31	[M+H]+	1		√	-0.25 ± 0.24**	-0.11 ± 0.24	
Others metabolites										
LPE (20:3)	502.2932	0.7	6.11	[M-H]-	2	√	√	-0.98 ± 0.83**	-0.66 ± 0.87**	**
LPE (18:3) or LPE (16:0)	476.2739	3.3	6.05	[M+H]+/ [M+Na]+	2	√	√	0.24 ± 0.42	0.36 ± 0.34***	**
LPE(16:1)	450.2596	3	5.82	[M-H]-	2	√	√	-0.55 ± 0.78**	-0.17 ± 0.59	
Palmitoylmonoglyceride	353.2650	1.2	6.32	[M+Na]+	1	√	√	-0.19 ± 0.33*	-0.03 ± 0.36	
Theobromine	181.0724	-0.4	3.57	[M+H]+	1		√	-0.86 ± 0.72**	-0.51 ± 0.91	
Indole-3-carboxaldehyde	144.0446	0.9	4.34	[M-H]-	1		√	-0.37 ± 0.48**	-0.59 ± 0.98**	**

Abbreviations: MU, Metabolically Unhealthy, MH, Metabolically Healthy; RT, Retention Time; sPLS-DA, Sparse Partial Least Squares Discriminant Analysis

a. Identified metabolites listed in according with metabolic classes and increasing the m/z of the compound.

b. Data obtained by LC-ESI-qTOF-MS.

c. Level of metabolite identification according to metabolomics Standard Initiative, Sumner et al.[27]

d. √ if the compound is discriminative between MH and MU in sPLS-DA analysis in the respective increments of time: T1-T0, T3-T0 and T6-T0

e. Values are shown as mean ± sd. Mean (log(T3)-log(T0)). *P* values were determined by paired *t*-test comparing T3 and T0 of each group after adjusted by gender, age and type of surgery and false discovery rate by Benjamini-Hochberg procedure. Total n 39 patients, separated in metabolically healthy (MH, n=21) and metabolically abnormal (MU, n=18) at baseline. At the different points of time the availability of the samples were: for MH 20, 20 and 17 and for MU: 16, 17 and 15 at 1 month, 3 months and 6 months respectively

f. *P* values were determined by independent *t*-test comparing MH at baseline vs MU 3 months of surgery after adjusted by gender, age and type of surgery and false discovery rate by Benjamini-Hochberg procedure.

* p<0.1, **p<0.05, ***p<0.001

Table 2. Enrichment analysis based on Chemical Similarity Enrichment Clustering performed by ChemRICH

Cluster name	Cluster size	MU			MH		
		Hits	Altered Ratio	*P*	Hits	Altered Ratio	*P*
Indole and derivatives	3	3	1	<0.001	2	0.7	0.068
Amino acids, peptides, and analogues	7	4	0.6	<0.001	1	0.1	1
Glycerolipids	5	4	0.8	0.001	0	0	1
Glycerophospholipids	3	2	0.7	0.002	2	0.7	0.076
Fatty Acyls	9	3	0.3	0.051	2	0.2	0.410

The significant clusters of metabolites generated by chemical similarity and ontology mapping by ChemRICH are shown. Hits mean the altered metabolites in metabolically unhealthy (MU) and metabolically healthy (MH) subjects, respectively. Chemical enrichment statistics was calculated by applying the Kolmogorov-Smirnov test on the 48 discriminant metabolites at the increment of time T3-T0. *P*-values were adjusted using the Benjamini-Hochberg method to control the false discovery rate.

Table of contents graphic (TOC)

For TOC only